

See discussions, stats, and author profiles for this publication at: <https://www.researchgate.net/publication/14325804>

Covalent structure of the flavoprotein subunit of the flavocytochrome c: Sulfide dehydrogenase from the purple phototrophic bacterium Chromatium vinosum

ARTICLE *in* PROTEIN SCIENCE · SEPTEMBER 1996

Impact Factor: 2.85 · DOI: 10.1002/pro.5560050901 · Source: PubMed

CITATIONS

19

READS

32

8 AUTHORS, INCLUDING:



Gonzalez Van Driessche

Ghent University

45 PUBLICATIONS 966 CITATIONS

[SEE PROFILE](#)



Moonjoo Koh

Chosun University

13 PUBLICATIONS 211 CITATIONS

[SEE PROFILE](#)



Francis Scott Mathews

Washington University in St. Louis

192 PUBLICATIONS 14,610 CITATIONS

[SEE PROFILE](#)



Covalent structure of the flavoprotein subunit of the flavocytochrome *c*: Sulfide dehydrogenase from the purple phototrophic bacterium *Chromatium vinosum*

GONZALEZ VAN DRIESENNE,¹ MONJOO KOH,^{1,4} ZHI-WEI CHEN,² F. SCOTT MATHEWS,² TERRY E. MEYER,³ ROBERT G. BARTSCH,³ MICHAEL A. CUSANOVICH,³ AND JOZEF J. VAN BEEUMEN¹

¹ Department of Biochemistry, Physiology and Microbiology, Laboratory of Protein Biochemistry and Protein Engineering, State University of Gent, B-9000 Gent, Belgium

² Department of Biochemistry, Washington University School of Medicine, St. Louis, Missouri 63110

³ Department of Biochemistry, University of Arizona, Tucson, Arizona 85721

(RECEIVED March 20, 1996; ACCEPTED April 14, 1996)

Abstract

The amino acid sequence of the flavoprotein subunit of *Chromatium vinosum* flavocytochrome *c*-sulfide dehydrogenase (FCSD) was determined by automated Edman degradation and mass spectrometry in conjunction with the three-dimensional structure determination (Chen Z et al., 1994, *Science* 266:430–432). The sequence of the diheme cytochrome *c* subunit was determined previously. The flavoprotein contains 401 residues and has a calculated protein mass, including FAD, of 43,568 Da, compared with a mass of 43,652 ± 44 Da measured by LDMS. There are six cysteine residues, among which Cys 42 provides the site of covalent attachment of the FAD. Cys 161 and Cys 337 form a disulfide bond adjacent to the FAD. The flavoprotein subunit of FCSD is most closely related to glutathione reductase (GR) in three-dimensional structure and, like that protein, contains three domains. However, approximately 20 insertions and deletions are necessary for alignment and the overall identity in sequence is not significantly greater than for random comparisons. The first domain binds FAD in both proteins. Domain 2 of GR is the site of NADP binding, but has an unknown role in FCSD. We postulate that it is the binding site for a cofactor involved in oxidation of reduced sulfur compounds. Domains 1 and 2 of FCSD, as of GR, are homologous to one another and represent an ancient gene doubling. The third domain provides the dimerization interface for GR, but is the site of binding of the cytochrome subunit in FCSD. The four functional entities, predicted to be near the FAD from earlier studies of the kinetics of sulfite adduct formation and decay, have now been identified from the three-dimensional structure and the sequence as Cys 161/Cys 337 disulfide, Trp 391, Glu 167, and the positive end of a helix dipole.

Keywords: amino acid sequence; glutathione reductase; protein mass spectrometry

Flavocytochrome *c*-sulfide dehydrogenase is found in both purple sulfur and green sulfur phototrophic bacteria, and is thought to function in sulfur metabolism (Cusanovich et al., 1991). FCSD has sulfide dehydrogenase activity *in vitro*, although the periplasmic location of the protein and the cytoplasmic location of sulfur granules suggest that this activity does not occur *in vivo* (Dolata et al.,

1993). Sulfide reduces the FAD, and electrons are passed on to the heme and eventually to a small soluble cytochrome *c*. The mechanism of FAD reduction is not yet known. The FCSD from the purple bacterium *Chromatium vinosum* differs from the green bacterial *Chlorobium thiosulfatophilum* FCSD in having a diheme rather than a monoheme subunit. The FAD is covalently bound to Cys 42 (Kenney & Singer, 1977; Van Beeumen et al., 1990, 1991).

FCSD has one of the highest known flavin redox potentials (−26 to +28 mV average two-electron potential), whereas the heme has one of the lowest potentials for type 1 cytochromes *c* (+15 to +93 mV) (Meyer et al., 1991a). The FAD of FCSD forms N-5 adducts with sulfite, thiosulfate, cyanide, and mercaptans (Cusanovich et al., 1991; Meyer et al., 1991b). This is probably due to the abnormally high redox potential of the flavin (Massey et al., 1969). A study of the kinetics of sulfite binding to the N5 position of the FAD as a function of pH suggested the presence of four

Reprint requests to: Jozef Van Beeumen, Vakgroep Biochemie, Fysiologie en Microbiologie, Universiteit Gent, Leeghwaterstraat 35, B-9000 Gent, Belgium; e-mail: vbeeumen@mgmicro.

⁴ Present address: Department of Chemistry, Chosun University, Kwangju, Seoul 501-759, Korea.

Abbreviations: AMP, adenosine monophosphate; ES, electrospray; FAD, flavin adenine dinucleotide; FCSD, flavocytochrome *c*-sulfide dehydrogenase; GR, glutathione reductase; MALDI, matrix assisted laser desorption ionization; MS, mass spectrometry; NAD(P), nicotinamide adenine dinucleotide (phosphate); PD, plasma desorption; RMSD, RMS deviation.

nearby functional groups (Meyer et al., 1991b). The high redox potential of the FAD, the stabilization of the anionic FAD semi-quinone, and the reaction with sulfite and other nucleophiles is likely to be due to a positive charge near the N1/O2 position of the FAD. It was postulated that either a lysine or arginine residue was involved. However, the three-dimensional structure shows that is actually the positive end of a helix dipole (Chen et al., 1994). Sulfite binding is accelerated below pH 7 in FCSD, whereas in other flavoproteins and in free flavin, sulfite is more reactive at high pH. Based on the observed pK of 6.5, the residue responsible for this effect was postulated to be a histidine, but it now appears from the crystal structure to be glutamate 167. In addition, the sulfite adduct forms a charge transfer complex with a functional group in the protein, which was postulated to be an aromatic residue such as tryptophan (Meyer & Bartsch, 1976), but is now thought to be tryptophan 391. At high pH, the sulfite adduct is unstable and decomposes with a pK of 8.5. This was postulated to be due to the reaction of sulfite with a disulfide bridge near the FAD. Ionization of the resulting free sulphydryl near the N1/O2 position of the FAD was postulated to neutralize the positive charge in that region, thereby lowering the redox potential of the FAD and causing decomposition of the N5 adduct (Meyer et al., 1991b). The disulfide is now known to involve cysteines 161 and 337, which are on the opposite side of the flavin from the disulfide present in glutathione reductase (Chen et al., 1994).

The amino acid sequences of the heme subunits of both flavocytochromes mentioned above have been determined (Van Beeumen et al., 1990, 1991). The subunit from *Chlorobium* FCSD is a small type I cytochrome *c* that is homologous to mitochondrial cytochrome *c*, although they are not particularly close to one another. The flavocytochrome *c* from *C. vinosum* contains two type I heme binding domains in the cytochrome subunit that exhibit an extremely low internal sequence similarity of only 7% to each other (Van Beeumen et al., 1991). The gene sequence of the *Chromatium* FCSD diheme subunit and part of the flavoprotein subunit show that they both have N-terminal leader sequences, indicating a periplasmic location for the functional FCSD (Dolata et al., 1993). The heme and flavoprotein subunit genes are adjacent and appear to form a single transcript. Unfortunately, the DNA restriction fragment only contained the first 95 residues of the flavoprotein subunit gene. Larger DNA fragments containing the whole FCSD operon and flanking genes were toxic to *Escherichia coli* and initial attempts to obtain the complete sequence of the flavoprotein gene failed. Thus, it was imperative to obtain the remainder of the sequence in order to complete the interpretation and refinement of the high-resolution three-dimensional structure. We now report the complete amino acid sequence of FCSD in conjunction with the X-ray crystallographic structure determination (Chen et al., 1994).

Results

The general strategy used for the sequence determination of the flavoprotein subunit of FCSD involved Edman degradation of peptide fragments obtained by digestion of the native or carboxymethylated apoprotein by several endopeptidases.

The first cleavage of flavoprotein subunit (Fig. 1), performed with Lys-C endoproteinase on the apoprotein, resulted in the peptides given in Figure 2. Edman degradation confirmed the already known N-terminal sequence (Dolata et al., 1993) and extended it up to residue 110. Overlaps between several Lys-C peptides were

obtained from the subsequent cleavage of the carboxymethylated apoprotein with Glu-C endoproteinase (Fig. 3) and Asp-N endoproteinase (Fig. S.I, Electronic Appendix). These allowed the N-terminal sequence to be extended to residue 168 and also identified residues 100 and 161 as cysteine. At this point, three fragments of the sequence beyond position 167 had been pieced together, ranging in size from 23 to 53 residues. These fragments were aligned individually with the 2.5-Å electron density map of the complete FCSD that had been fitted previously with the cytochrome subunit and the first 168 residues of the flavoprotein subunit (Chen et al., 1994). Overlaps between the fragments were further developed by additional sequencing of peptides using feedback from the X-ray derived overlaps and correlations between amino acid identity and electron density side-chain shape.

Thus far, four gaps in the sequence ranging from 6 to 25 residues in length remained and the identities of a number of amino acids required verification. The sequences of several Asp-N peptides (nD23/24, nD F5) filled the gap between fragments 4 and 1 and revealed the residues 274 and 296 to be cysteines. Also, the extension of the C-terminal fragment (fragment 1 in Fig. 1) to position 401, indicated by the Glu-C peptide S22A, was confirmed by peptide nD G4. The overlap between the N-terminal region 1–203 and the C-terminal region 236–401 was obtained through a final digest of the carboxymethylated apoprotein with Arg-C endoproteinase (Fig. S.II, Electronic Appendix) yielding peptide R19B. The overlap in the region 202–204 remained a bit weak from the sequence data, but was strongly confirmed from the mass data of the concerned peptides S10B, S11B, and K23A. At this point, only the residues 321 and 337 remained to be determined. The former was identified from a peptide of 11 residues that had been missed during the direct separation of the Lys-C digest by RP-HPLC but that was recovered from a prior separation of the digest by gel filtration (Fig. S.V and VI, A–E, Electronic Appendix). Residue 337 was never identified directly by sequence analysis but could be deduced from the ESMS spectrum of peptide nD23 to be carboxymethylcysteine. The mass of 6,663.1 Da for this peptide corresponds to the calculated value of 6,662.5 Da if one assumes that the methionine residue in this peptide (Met 301) was also carboxymethylated. This type of derivatization of methionine has been reported in the literature (Gurd, 1972) and was also found during the present sequence determination in the peptides S15A, S15B, S23, and nD16. The placement of nearly all of the cysteine residues, as well as of the methionine residues, was independently verified by a strong correlation between their positions and the major peaks in the anomalous scattering difference electron density map of the native protein. This approach has been used successfully in other examples of combined X-ray and chemical sequence studies of proteins (Barber et al., 1992). The final evidence for the C-terminal sequence of the flavoprotein subunit polypeptide chain was provided by mass analysis of several C-terminal peptides such as S22A and nD F2.

Concerning the specificity of the proteolytic enzymes used, we should mention that several different nonspecific cleavages have been found: K5 and K6 at Met at K7 at Ser. We also observed cleavages of Asp-X instead of normal Glu-X peptide bonds in peptides S3, S5, S7, S10B, S13, S17A, and S21B, even though digest conditions have been used that are generally believed to cleave peptide bonds only at the C-terminal side of glutamic acid.

Following completion of the amino acid sequence, the structure of FCSD was refined to an *R*-factor of 0.226 in the resolution range 8–2.53 Å, with no solvent added. The RMSD in bond lengths and

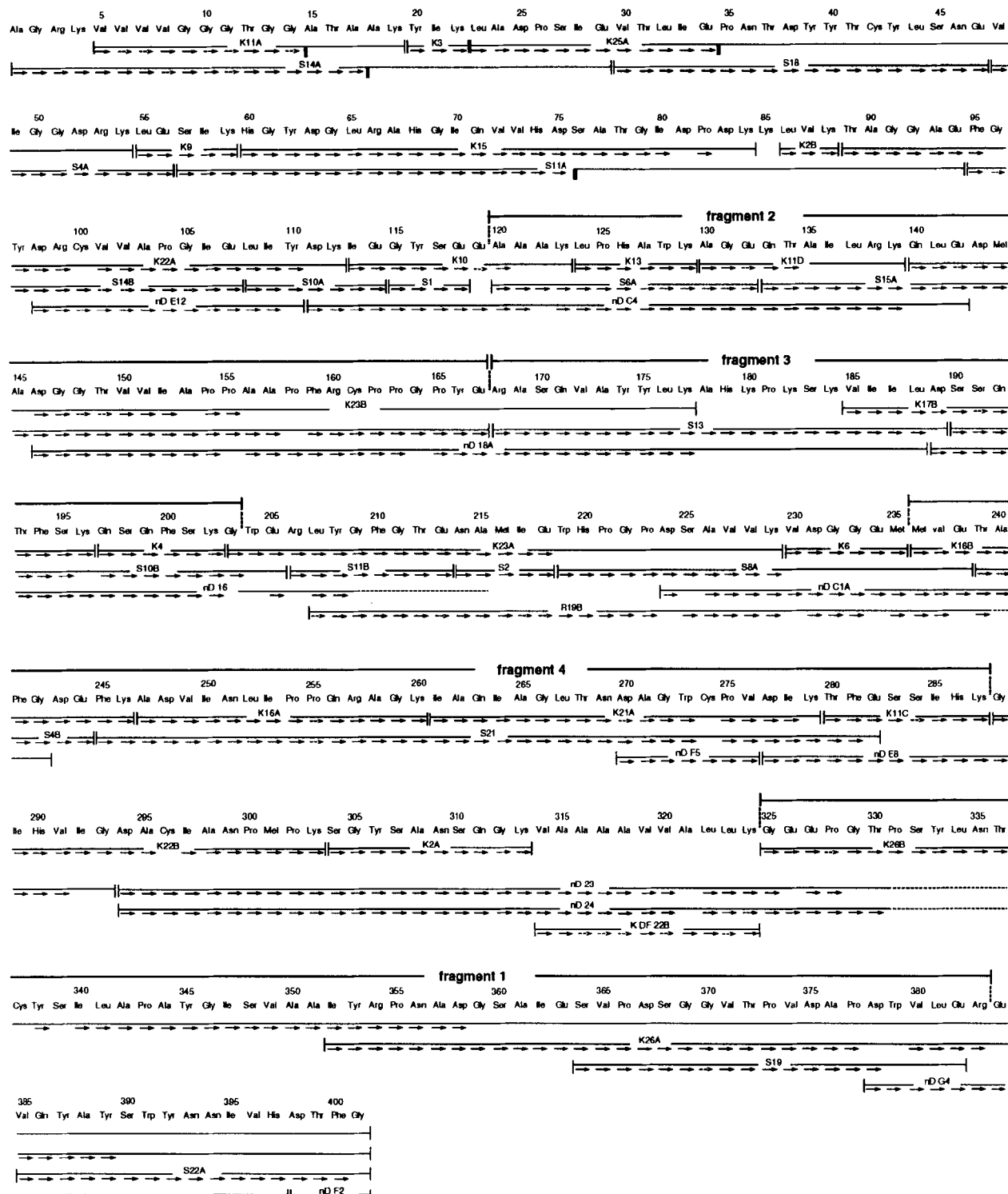


Fig. 1. Amino acid sequence of the flavoprotein subunit of *C. vinosum* FCSD. Evidence for this sequence comes from Edman degradation of peptides obtained from digestions with Lys-C endopeptidase (K), Glu-C endopeptidase (S), and Asp-N endopeptidase (nD). The cysteines were identified as carboxymethylcysteine after modification of the apoprotein. Sequence runs that were deliberately stopped are indicated by a black rectangle. Lines above the sequence, with the expression "fragment," represent those parts of the sequence that were used for simplifying the description of results.

angles from ideal values were 0.016 and 3.5 degrees, respectively. The four discrepancies between the electron density and the partial sequence mentioned previously (Chen et al., 1994) are now re-

solved. In two of the cases, Cys was misidentified in the sequence as Ser; in the other two, a Lys was misidentified as Met and a Val was misidentified as Ala.

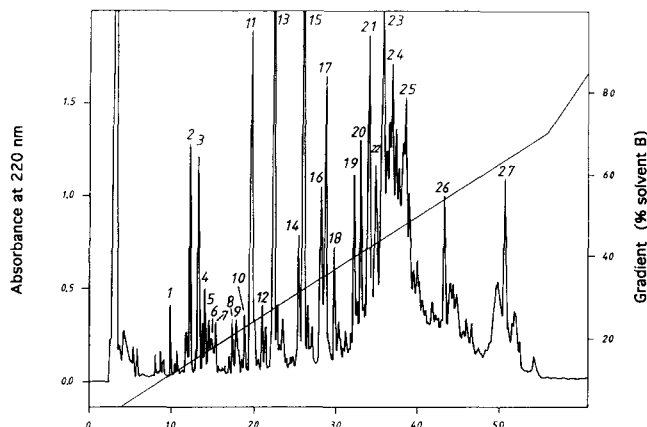


Fig. 2. Reversed phase HPLC of peptides from digestion of apoprotein with Lys-C endoproteinase. Conditions for the separation are described in Materials and methods.

Discussion

Sequence evidence

The complete primary structure of the flavoprotein subunit of FCSD from *C. vinosum* is presented in Figure 1. Evidence for this sequence was obtained from N-terminal sequence analyses of overlapping peptides obtained from different enzymatic digestions. The first 95 residues were already established by both protein sequence (Van Beeumen et al., 1991) and nucleotide sequence determinations of a 2.6-kb DNA restriction fragment (Dolata et al., 1993). Large peptide fragments were fitted into the electron density map of the flavoprotein subunit, which aided in locating further overlaps. With the support of accurate mass data for most of the sequenced peptides, we consider each residue in the proposed sequence of the flavoprotein subunit of FCSD to be proven solidly.

The mass of the native protein could not be measured by ESMS under the conditions given in Materials and methods, but MALDI-MS did reveal a value of 43,652 Da (Fig. 4). The calculated sum of the masses of the amino acid residues (without disulfide bridges but with FAD) is 43,568 Da, indicating a mass difference of 84 Da. This is outside the generally assumed accuracy of the LDMS method (0.1%). It is possible that this discrepancy comes from a sulfite bound to either FAD or to the disulfide (McPhee, 1956; Muller & Massey, 1969; Meyer et al., 1991a, 1991b), although no spectral evidence supports this assumption and no such molecule was observed in the crystallographic structure. However, since we and others often observe that methionines and, in some cases, tryptophans get oxidized during purification of peptides, it is possible that the discrepancy arises from such a modification. This might not be visible in the structure when oxidation of each susceptible residue is prevented during crystallization. Agreement between the calculated and the measured masses for all the peptides, including the firm identification of the N- and C-terminal residues, and the electron density map (Chen et al., 1994) all clearly indicate that there are exactly 401 residues in the mature flavoprotein subunit of FCSD. Our amino acid composition analysis (Table S.XI, Electronic Appendix) is in good agreement with the calculated composition, but is divergent from the one reported in the literature (Yamanaka et al., 1976).

Fig. 4. Matrix assisted laser desorption mass spectrum of native flavoprotein subunit (43,652 Da). The peaks of 33,216 and 66,428 Da are from the internal standard (bovine serum albumin) to calibrate the spectrum.

It was established previously that the co-factor FAD is covalently attached via a thioether bridge from the 8-methyl group of FAD to a cysteine residue (Kenney & Singer, 1977), now known to be at position 42 (Van Beeumen et al., 1990, 1991). There are five additional cysteines in the protein, at positions 100, 161, 274, 296, and 337. All six cysteines were identified as the carboxymethyl derivative after modification of the apoprotein. From comparison with the three-dimensional structure, we can now firmly state that cysteines 161 and 337 are linked by a disulfide bridge and are adjacent to the flavin (Chen et al., 1994). The alpha carbons of Cys 274 and Cys 296 also are close enough for these two residues to form a disulfide, but the three-dimensional structure shows that the sulfur atoms are oriented in a way such that they are actually too distant to form such a bridge, and that they are distant from the flavin as well.

FAD binding fingerprint sequences in relation to the GR family of flavoproteins

We have shown previously that the N-terminal region of the flavoprotein subunit of FCSD is homologous to a number of flavoproteins, including succinate dehydrogenase, fumarate reductase, lipoamide dehydrogenase, and GR (Van Beeumen et al., 1991). This allowed us to refine the previously derived fingerprint for

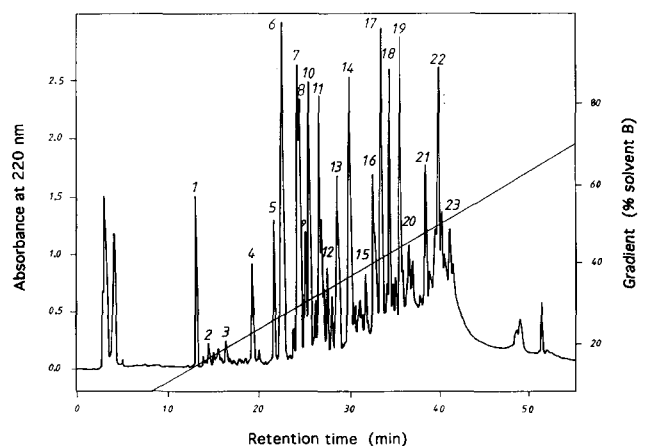


Fig. 3. HPLC separation pattern for peptides obtained after digestion of the carboxymethylated apoprotein with Glu-C endoproteinase. Conditions are described in Materials and methods.

FAD binding (Wierenga et al., 1986) within the larger family of flavoproteins that adopt the Rossmann fold (Rossmann & Argos, 1978). This $\beta\alpha\beta$ -nucleotide fold is also found in the pyridine nucleotide-dependent dehydrogenases (homologous to the prototypic lactate dehydrogenase) that have a very similar sequence fingerprint. In the following paragraph, we propose a refinement of the FAD fingerprint for the family of flavoproteins more closely related to GR, of which FCSD is a member.

The three-dimensional structures of members of the GR family are characterized by five parallel strands and three antiparallel beta strands situated between the third and fourth parallel strands, as exemplified by the structure of the prototypic GR (Thieme et al., 1981). A conserved helix is located between the first and second strands. The fifth parallel strand comes from a discontinuous section of peptide chain sometimes referred to as the "central domain" (see below). The pyridine nucleotide-dependent dehydrogenases contain six contiguous parallel beta strands with connecting helices and lack the three antiparallel beta strands characteristic of the GR family. The three-dimensional structure shows that the flavin subunit of FCSD is spatially homologous to the GR family of flavoproteins in its entire length (Chen et al., 1994).

In addition to the Wierenga et al. (1986) fingerprint in the N-terminal $\beta\alpha\beta$ -region, which is characteristic for the FAD binding proteins in general, Eggink et al. (1990) have identified another fingerprint, which is specific for the GR family of proteins, that includes the fifth parallel beta strand in the central domain. In Figure 5, we have aligned the fingerprint regions of the 15 functionally different members of the GR family of flavoproteins. We have simplified the fingerprints by excluding residues that are not as well conserved as the others and those that are disconnected

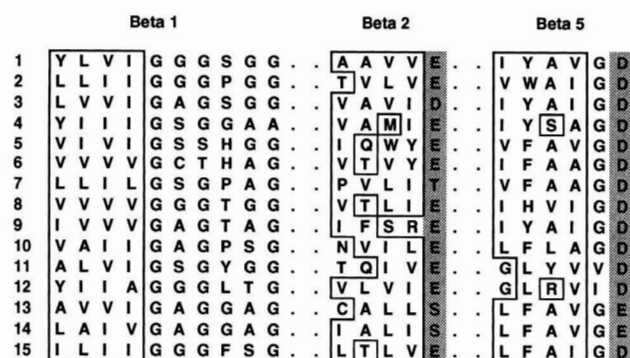


Fig. 5. FAD-binding sequence fingerprint of the GR family of flavoproteins adapted from Wierenga et al. (1986) and Eggink et al. (1990). The fingerprint is divided into three segments that are labeled according to their positions in the structure. Proteins are ranked according to the extent of similarity to GR. 1, Human GR (Krauth-Siegel et al., 1982); 2, *Pseudomonas putida* lipoamide dehydrogenase (Burns et al., 1989; Mattevi et al., 1992); 3, *Critchidia fasciculata* trypanothione reductase (Hunter et al., 1992); 4, *Bacillus* sp. mercuric ion reductase (Wang et al., 1989); 5, *Streptococcus faecalis* NADH peroxidase (Ross & Claiborne, 1992); 6, *S. faecalis* NADH oxidase (Ross & Claiborne, 1992); 7, *E. coli* thioredoxin reductase (Kuriyan et al., 1991b); 8, *C. vinosum* flavocytochrome c-sulfide dehydrogenase (this work); 9, *Pseudomonas oleovorans* rubredoxin reductase (Eggink et al., 1990); 10, p-hydroxybenzoate hydroxylase (Weijer et al., 1982); 11, *Brevibacterium sterolicum* cholesterol oxidase (Fujishiro et al., 1990; Vrielink et al., 1991); 12, *Aspergillus niger* glucose oxidase (Frederick et al., 1990); 13, *E. coli* succinate dehydrogenase (Wood et al., 1984); 14, *E. coli* fumarate reductase (Burland et al., 1995); and 15, *Archaeoglobus* adenosine phosphosulfate reductase (Speich et al., 1994). The hydrophobic residues of the fingerprint are boxed and residues that hydrogen bond the FAD ribose and the ribityl side chain are highlighted by a grey background.

Table 1. Some specific structural features of the GR family of flavoproteins^a

	Amino acids near the flavin and pyridine nucleotide				Special features								
	A	B	C	D									
GR	E58	C63	K67	Y197	D220	D331	H467'	100	0	100	+	C58-C63, located at <i>si</i> ^b face of FAD	
LD	E32	C40	C45	K49	Y178	E201	H434'	25	+	+			
TR	D35	C52	C57	K61	F198	E202	D327	37	14	80	+	C628'-C629' binds mercury, along with Y605' and Y264	
MR	E199	C207	C212	(K216)	Y344	E348	D472	Y605'	25	+	+	C42 oxidized to sulfenic acid; H10 also functions in catalysis	
NP	E32	C42	E32	C42	(K51)	Y159	E163	D281	15	18	58	+	
NO								D280					
TRR		T35				E159	E161		18	13	43	-	NADPH domain rotated relative to the FAD domain; no obvious binding site for thioredoxin. C135-C138, located at <i>re</i> ^b face of FAD
PHBH		E32					D286		6	14	-		
CO		E41				E167	D294						
GO		E50					D441						
FCSD		E34	C42										
APSR		E56											

^a Column A, sequence identity to other sequences of GR family (approximate %); column B, insertions and deletions, compared with GR structure; column C, spatial equivalency to GR structure (approximate %); column D, interface domain between two subunits; (), indicates a nearby but not strictly homologous residue; GR, glutathione reductase; LD, lipoamide dehydrogenase; TR, trypanothione reductase; MR, mercuric reductase; NP, NADH peroxidase; NO, NADH oxidase; TRR, thioredoxin reductase; PHBH, p-hydroxybenzoate hydroxylase; CO, cholesterol oxidase; GO, glucose oxidase; FCSD, flavocytochrome c-sulfide dehydrogenase; APSR, adenosine phosphosulfate reductase.

^b When viewed from the *si* face, the ribityl side chain points up and the pyrimidine ring is on the right.

from the main segments. We also divided the Wierenga et al. (1986) fingerprint into two similar segments, which we labeled beta 1 and beta 2, according to their predominant secondary structure and position in the structure. The Eggink et al. (1990) fingerprint is similar in composition to that of Wierenga et al. and contains an extra element, labeled as beta 5, according to its location. Each of these three fingerprint elements generally contain four hydrophobic residues in a row, of which valine, isoleucine, and leucine are the most prevalent. The four beta 1 hydrophobic residues are immediately followed by five conserved glycine (or small amino acid) residues in the sequence GGGXGG. The first, central, and last glycine residues are usually the most highly conserved. These glycines allow close packing of the dinucleotide and position the pyrophosphate over the N-terminus of the first helix, the positive dipole of which partially neutralizes the negative charge of the pyrophosphate. The beta 2 fingerprint is separated from beta 1 by 13–17 residues, which include the first alpha helix. The four hydrophobic residues are immediately followed by a Glu, Asp, Thr, or Ser, which hydrogen bond the FAD ribose. The second residue of the β 2-fingerprint is occasionally a Thr, which then also hydrogen bonds the ribose. The beta 5 fingerprint is usually separated from the first two by about 250–280 residues, a region that in most cases includes the pyridine nucleotide-binding domain. The four hydrophobic residues of the beta 5 fingerprint are immediately followed by the sequence Gly Asp/Glu. The acidic residue functions to hydrogen bond the ribityl side chain of FAD. The second residue of this fingerprint element is often aromatic.

The pyridine nucleotide-binding domains in the GR family of flavoproteins are generally more closely related to the FAD-binding domain of this family than to the other nucleotide-binding proteins having the Rossmann fold. In other words, both domains have four parallel beta strands with three antiparallel strands between the third and fourth parallel strands, but the pyridine nucleotide binding domains lack the beta 5 fingerprint characteristic of the FAD binding domains.

Active site comparisons and evolutionary relationships within the GR family

The overall similarity among the GR family of flavoproteins is more apparent from the three-dimensional structures than from the

amino acid sequences. In fact, the only easily recognized segment of the sequence is the 21-residue fingerprint described above, especially the four hydrophobic residues followed by five glycines in beta 1 at the beginning of the Rossmann fold. The similarity among the most divergent proteins of the family averages about 10–20%. In addition, insertions and deletions occur too frequently to provide more than a qualitative measure of relationships within this family of proteins. Amino acid residues and functional groups near the flavin and pyridine nucleotide that affect their properties and that are involved in catalysis are more revealing of the relationships among these proteins. Nevertheless, the number of spatially equivalent residues found by comparing the three-dimensional structures may provide the best quantitative indication of relationships. The following descriptions of the major proteins in the family place FCSD in perspective as being one of the most divergent members. The main features of the individual proteins are summarized in Table 1.

Among those flavoproteins for which the three-dimensional structures are known, GR (Thieme et al., 1981; Karplus & Schulz, 1987, 1989; Mittl & Schulz, 1994), lipoamide dehydrogenase (LD) (Mattevi et al., 1991, 1992), and trypanothione reductase (TR) (Shames et al., 1988; Kuriyan et al., 1991a; Hunter et al., 1992; Lantwin et al., 1994) are the most closely related. Virtually all the amino acid residues spatially nearest to the flavin and pyridine nucleotide are conserved. The helix starting at position 339 from the central domain, which is at the N1/O2 position of FAD, is also spatially conserved, although it is not possible to identify it from the sequence alone. The sequences of various species of TR are approximately 37% identical to those of GR. There are 421 equivalent residues of 478 and 491 residues. This corresponds to approximately 80% spatial equivalency. LDs are only slightly more divergent, with an average 25% sequence identity to either GR or TR.

Mercuric reductase (MR) (Schiering et al., 1991) is somewhat more divergent than the above. Although it has the homologous active site residues, there is an additional disulfide (C628'–C629') that, in the reduced form, functions in part to bind mercury. H467' from the adjacent subunit and at the interface domain of GR is replaced by Y605' in MR which, along with Y264, also functions in metal binding (Schiering et al., 1991). The mercuric reductases average about 25% identity to GR, TR, and LD.

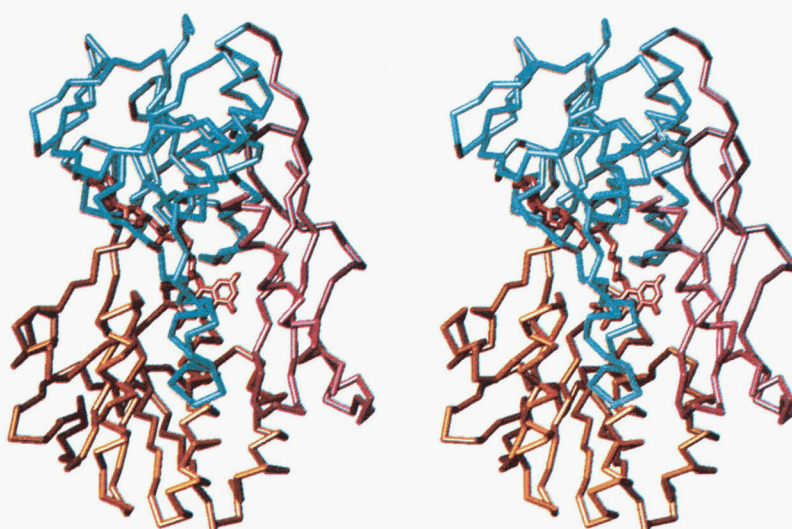


Fig. 6. Stereo diagram of the flavoprotein subunit of FCSD. The $C\alpha$ backbones of domains 1, 2, and 3 are colored blue, gold, and magenta, respectively. The FAD molecule is shown in red. In the sequence figure (Fig. 7), the three domains are colored similarly.

In NADH peroxidase (NP) and the closely related NADH oxidase (NO) (Stehle et al., 1991; Ross & Claiborne, 1992; Liu & Scopes, 1993), there are fewer active site residues present. Only the first of the two active site cysteines (C42) is retained. It is oxidized to sulfenic acid by peroxide and oxygen. H10, a nonconserved residue in the beta 1 FAD fingerprint region, also functions in catalysis. In a comparison of the three-dimensional structures of

GR and NP, there are only 301 equivalent residues of 478 and 447, respectively (corresponding to approximately 58% spatial equivalency). Thus, NP and NO are somewhat more divergent than is mercuric reductase.

Thioredoxin reductase (TRR) (Waksman et al., 1994) is even more dissimilar in lacking the 130-residue interface domain and the disulfide in the flavin domain. Instead, it has a disulfide (C135/

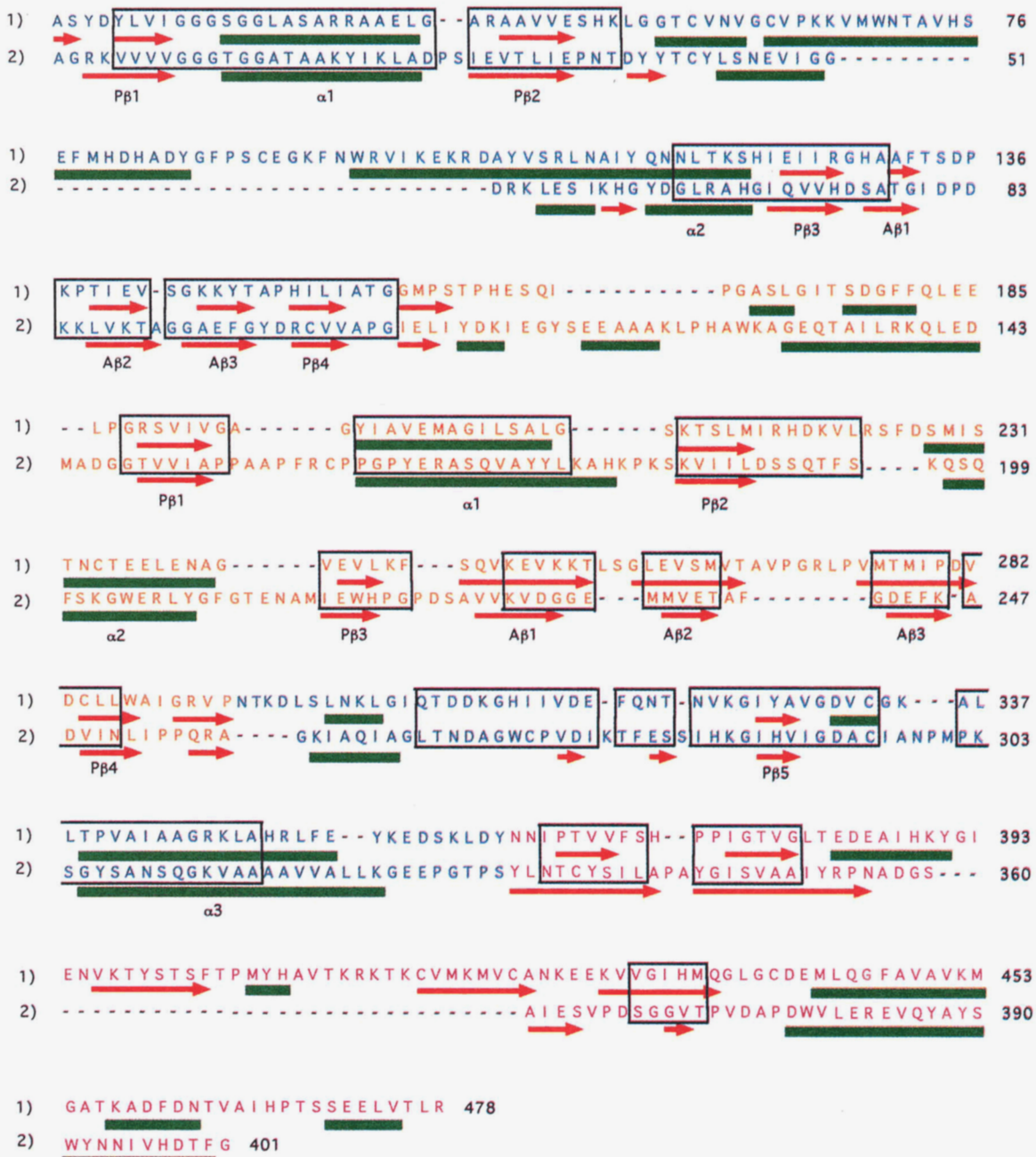


Fig. 7. Alignment of the sequences of human GR (1) (Krauth-Siegel et al., 1982) with *C. vinosum* FCSD flavoprotein subunit (2) (this work) based on superposition of the three-dimensional structures shown in Figure 8 (Schulz et al., 1992; Chen et al., 1994). Secondary structures in both cases were assigned using the program STRIDE (Frishman & Argos, 1995). Structurally equivalent residues, identified as described in the text, are enclosed in boxes. Helical segments are indicated in green bars, and beta sheets in red arrows under the sequences. The three domains of the two proteins are represented by different letter colors: domain 1, blue; domain 2, orange; domain 3, purple. The major secondary structural elements of the core α/β motifs in domains 1 and 2, characteristic of the prototypical GR fold (see text), are labeled P_{Bn}, A_{Bn} and α n for the parallel beta strand, antiparallel beta strand, and alpha helices, respectively. The first two antiparallel β strands of the interface domain of GR are also indicated. The first 18 residues of GR have no comparable region in FCSD and are disordered in the electron density map; they have therefore been omitted.

C138) located in the NADPH domain on the opposite face of the FAD as in GR. D139, which has no counterpart in the other proteins, is involved in catalysis as well. The central domain helix at the N1/O2 position of the FAD is present. The NADPH domain is rotated relative to the FAD domain and there is no obvious binding site for thioredoxin, suggesting rearrangement during catalysis. There is only about 18% sequence identity to the above proteins. Comparison of the three-dimensional structures of GR and TRR shows that there are only 211 equivalent residues of 320 in TRR, which corresponds to approximately 43% spatial equivalency.

The FAD domain of para-hydroxy-benzoate hydroxylase (PHBH) (Wierenga et al., 1983) is homologous to the FAD domain of the GR family of flavoproteins, although the NADPH domain is not related. There is virtually no similarity at the active site except for the 21-residue fingerprint and the stabilizing helix dipole located at the N1/O2 position of the FAD. The interface domain is absent.

Cholesterol oxidase (CO) (Vrielink et al., 1991) and glucose oxidase (GO) (Hecht et al., 1993) are both more closely related to PHBH than to the other proteins in that they have only the GR family FAD fingerprint. In comparing the three-dimensional struc-

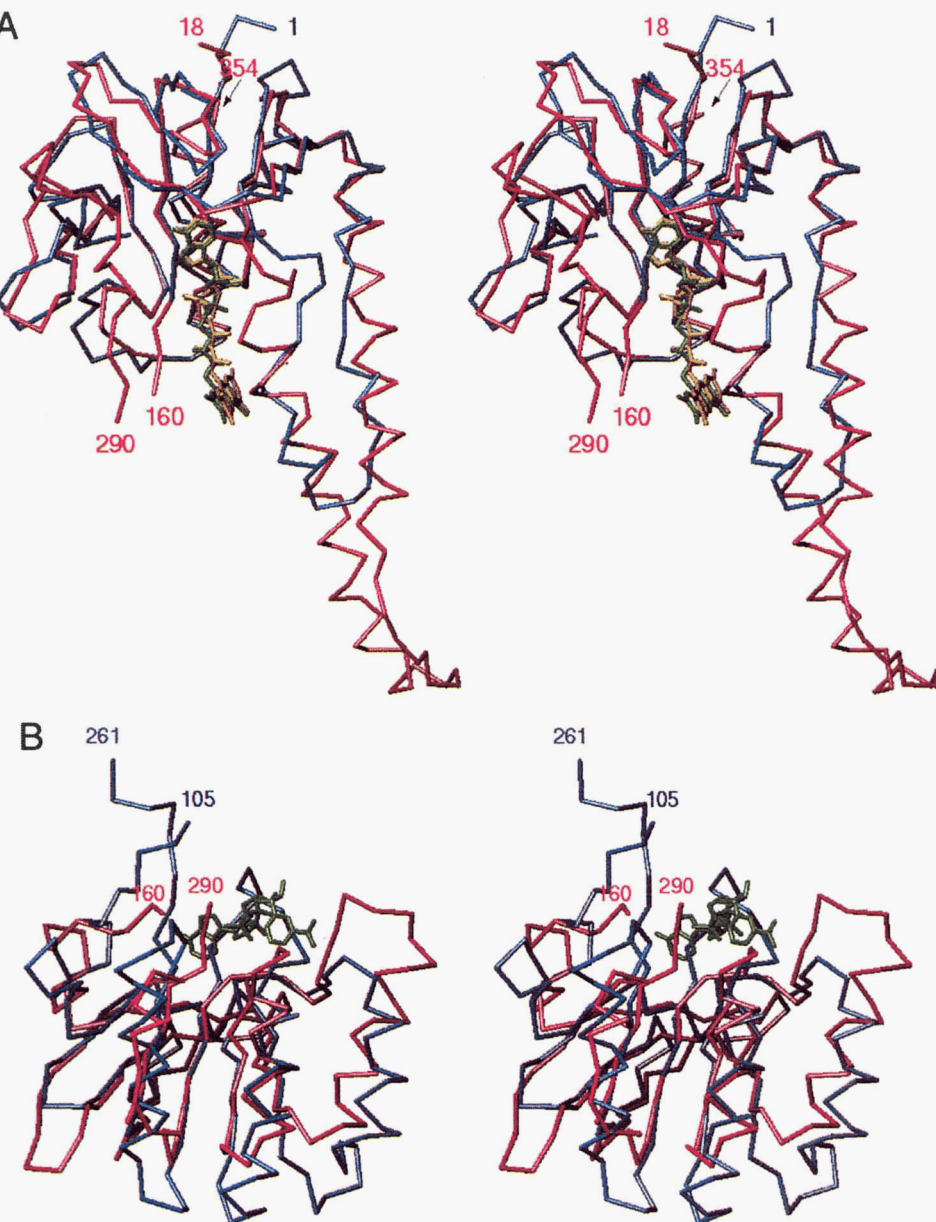
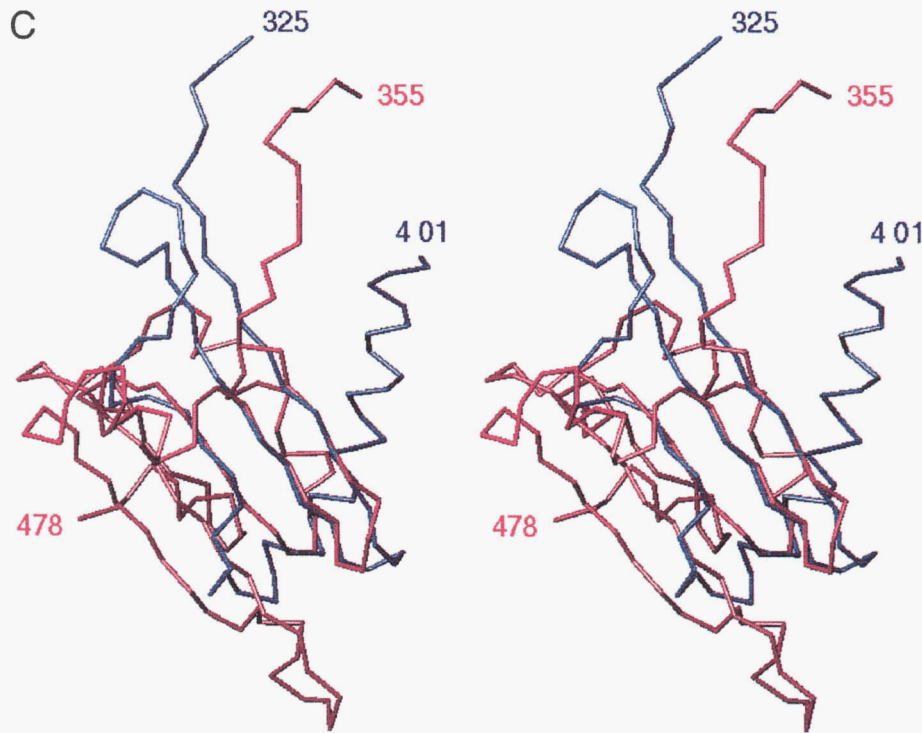


Fig. 8. Stereo diagram of the three separate domains of GR superimposed onto the corresponding domains of FCSD. The α -backbones of GR and FCSD are magenta and blue, respectively, and the FAD and NADPH (for GR only) prosthetic groups are green and yellow, respectively. **A:** FAD binding domain, consisting of residues 18–157 and 294–357 of GR and residues 1–105 and 259–325 of FCSD (not labeled). The RMSD of 114 equivalent α -atoms separated by 2.0 Å or less is 1.07 Å. **B:** NADPH binding domain of GR (residues 158–293) and domain 2 of FCSD (residues 106–258). The RMSD of 75 equivalent α -atoms separated by 2.0 Å or less is 1.24 Å. In FCSD, the second parallel β -strand and the following α -helix extend further than in GR, so that the position of NADPH in GR is occupied in FCSD by the heptapeptide segment from Pro 155 to Cys 161. **C:** Domain 3 of GR (residues 358–478, the “interface domain”) and FCSD (residues 326–401). The RMSD of 24 equivalent α -atoms separated by 2.0 Å or less is 1.06 Å. (*Figure continues on facing page.*)

Fig. 8. *Continued.*

tures of GR and PHBH, there are only 90 equivalent residues, corresponding to approximately 14% spatial equivalency. This group of proteins is significantly more divergent than TRR.

In the context of the above discussion, FCSD (Chen et al., 1994) is at least as divergent as TRR, but not as much as PHBH. The overall fold of the FCSD flavoprotein subunit is shown in Figure 6. FCSD contains the 21-residue FAD fingerprint and both FAD and NAD domains, but the interface domain is truncated to provide a binding site for the cytochrome subunit. The sequence alignment of FCSD and GR is shown in Figure 7, based on separate superposition of each of the three domains of GR and FCSD as shown in Figure 8 (Thieme et al., 1981; Karplus et al., 1987, 1989; Chen et al., 1994). Note that domain 1 is composed of two noncontiguous segments of peptide chain, the N-terminal segment, and what used to be called the central domain, located between domains 2 and 3. The orientation of domain 2 with respect to domain 1 differs by about 9.5 degrees compared with GR. The position of domain 3 with respect to domain 1 also differs by both 6 Å translation and 14.3 degrees rotation compared with GR.

The GR disulfide is absent in FCSD, but there is a disulfide on the opposite side of the FAD (C161/C337), which is not homologous to that of TRR either. FCSD C42, which is in the vicinity of the GR disulfide, actually provides the site of covalent binding of the FAD. Those acidic residues in the GR family that hydrogen bond the FAD ribose and ribityl side chain are present (E34 and D294), as is the stabilizing helix from the central domain, which interacts with the N1/O2 position of the FAD. GR E201, which is near the N5 position of FAD, is present in FCSD as E167, but the basic residue that should charge pair with it is absent. Those proteins in the family that interact with NAD (such as LD and NP) have an acidic residue at the end of the beta 2 pyridine nucleotide fingerprint that hydrogen bonds the NAD ribose. Those that bind NADP have two arginines in this region (such as in GR, TR, MR,

and TRR). FCSD has an Asp in this position, which suggests that if it interacts with nucleotides at all it would be specific for NAD rather than for NADP. Because the disulfide blocks access to the FAD (see Fig. 8), FCSD shares the same dilemma as TRR in that a conformational change would have to occur to allow pyridine nucleotide to bind in the usual manner as for other members of the family. Consistent with this observation is the fact that FCSD is not very reactive with pyridine nucleotides. This does not exclude the possibility that FCSD may bind AMP by analogy with APS reductase (see below). In fact, there is a large cavity leading to the disulfide that would allow interaction with soluble cofactors. FCSD shows only about 12% sequence identity with members of the greater GR family of proteins. In comparison of the three-dimensional structures of GR and FCSD, at least 20 internal insertions and deletions ranging in size from 1 to 37 residues are apparent and there are 188 equivalent residues, which corresponds to approximately 36% spatial equivalency.

Adenosine phosphosulfate reductase (APSR) is the second of three enzymes in both assimilatory and dissimilatory pathways for sulfate reduction to sulfide. The sequence of *Archaeoglobus* APSR was shown to be homologous to succinate dehydrogenase and fumarate reductase throughout its length (Speich et al., 1994). In addition, it has all three fingerprint sequences typical of the GR family of proteins. It is at least as divergent as TRR and FCSD, but not as much as PHBH. It does not have any of the three types of disulfides found in GR, TRR, or FCSD, and any of the other active site residues near the flavin in GR. The fingerprint for the domain 2 pyridine nucleotide binding site is present, but appears to be located earlier in the sequence than suggested by Speich et al. (1994). It probably functions to bind adenosine monophosphate (AMP) and APS. We postulate that the second domain in FCSD may bind AMP to catalyze a reaction in the reverse direction as occurs in APSR, that is, oxidation of thiosulfate and sulfite to APS.

FCSD is a soluble periplasmic protein and may not be the principal sulfide dehydrogenase in vivo. This role is probably taken by a membrane-bound sulfide-quinone oxidoreductase flavoprotein, as is found in *Oscillatoria limnetica* and *Rhodobacter capsulatus* (Arieli et al., 1994). The N-terminal sequence of this enzyme shows that it has the first of the two FAD binding fingerprints. There is a strong possibility that it is homologous to FCSD and APSR, suggesting that all the flavoprotein enzymes known to be involved in sulfur chemistry may be related.

Cytochrome binding

It has already been fully described in Chen et al. (1994) that the first heme domain of the diheme cytochrome subunit binds to domain 3 of the flavoprotein subunit through 13 hydrogen bonds and one salt bridge.

Materials and methods

Protein modification

Reduction of 10 nmol of native flavoprotein subunit was performed overnight at 37 °C with dithiothreitol in 100 mM ammonium bicarbonate buffer, pH 8. The reduction mixture was then desalted by gel filtration over a BioRad SG 25 column (1 × 13 cm), equilibrated, and eluted with 0.1 M ammonium bicarbonate, pH 8.

Native flavoprotein subunit (60 nmol) was reduced with dithiothreitol in 50 mM phosphate buffer, pH 7.1, containing 50 mM EDTA and 6 M guanidine hydrochloride. The reaction mixture was flushed with argon and incubated for 7 h at 37 °C. Carboxymethylation as described by Crestfield et al. (1963) was performed after cooling the reaction mixture in an ice-bath for 30 min. The reduced protein was then carboxymethylated with 2.5 mM iodo acetic acid and incubated overnight at room temperature. Desalting was performed by gel filtration on a Superdex 75 PC 3.2/30 column (Pharmacia SMART-system, Uppsala, Sweden), equilibrated, and eluted with 10 mM ammonium hydrogen carbonate, pH 7.8.

Enzymatic digestions

Digestion with Lys-C endoproteinase from *Achromobacter lyticus* (Wako, Osaka, Japan) was performed on 10 nmol of apoprotein using an E/S ratio of 1/100 (weight/weight) in 100 mM Tris-HCl buffer, pH 8.0, at 37 °C for 4 h. Glu-C endoprotease (Boehringer, Mannheim, FRG) digestion was performed on 12.5 nmol carboxymethylated apoprotein in 100 mM ammonium hydrogen carbonate, pH 7.8, at 37 °C for 4 h, using an enzyme to substrate ratio of 1/40 (w/w). Carboxymethylated apoprotein (12.5 nmol) was digested with Asp-N endoproteinase from *Pseudomonas fragi* (Sigma, St. Louis, Missouri) in 100 mM ammonium hydrogen carbonate buffer, pH 7.8, for 4 h at 37 °C, using an enzyme to substrate ratio of 1/275 (w/w). An Arg-C endoproteinase (Boehringer, Mannheim, FRG) digestion was conducted on 7.5 nmol of carboxymethylated apoprotein at an E/S ratio of 1/45, in 0.01 M ammonium hydrogen carbonate, pH 8.0. The incubation time was 4 h at 37 °C.

Peptide and protein purification

Peptides obtained after different enzymatic digestions were separated by HPLC on a μRPC C2/C18 PC 3.2/3 or a μRPC C8 PC 2.1/10 column (Pharmacia SMART-system). The eluents were 0.05% TFA in MQ-water (solvent A) and 0.045% TFA in 70% acetonitrile

(solvent B). The digestion mixture from the Lys-C and Asp-N digestion of the apoprotein and carboxymethylated protein, respectively, were also separated by gel filtration on Superdex 30 PC 3.2/30 (Pharmacia SMART-system), equilibrated, and eluted with 50 mM ammonium hydrogen carbonate, pH 7.8. Fractions were further chromatographed by RP-HPLC on the above described columns, using the same elution conditions.

Amino-terminal sequence and amino acid composition analysis

Automated N-terminal sequence analysis of peptides were performed either with an Applied Biosystems pulsed liquid 475A, 477A, and/or 476A sequenator, equipped with an on-line (475A and 477A) or built-in 120A PTH-amino acid analyzer (476A).

Amino acid composition analysis was performed on a 420A Derivatizer (Applied Biosystems) with an on-line 130A Separation System (Applied Biosystems). Gas phase hydrolysis at 106 °C for 24 h was performed in a borosilicate glass tube of 5 × 55 mm placed in a Pierce hydrolysis vial, using 6 N HCl as hydrolysis agent.

Mass analysis

Plasma desorption mass spectra were collected on a Biolon 20K Biopolymer Mass Analyzer (Biolon, Uppsala, Sweden) during 10⁶ counts of the ²⁵²Cf source at an accelerating potential of 15 kV. Samples were applied in small volumes of 0.1% TFA in Milli-Q water and spin-dried on nitrocellulose coated targets wetted with 5 μL 0.1% TFA in methanol.

Electrospray mass spectrometry was performed on a Bio-Q quadrupole mass spectrometer equipped with an electrospray ionization source (Fisons Instruments, Altringham, UK). Ten microliters of sample solution in 50% acetonitrile/1% acetic acid were injected manually in the 10-μL loop of the Rheodyne injector and pumped to the source at a flow rate of 5 μL/min. The solvent, 50% acetonitrile/1% acetic acid, was delivered by a 140A Solvent Delivery System (Applied Biosystems). Scans of 12 s over the mass range of 400 to 1,600 a.m.u. were collected over 2 min. Calibration of the scans was performed with 50 pmol of horse heart myoglobin (Sigma).

MALDI-MS was performed on a ToFSpec instrument using a nitrogen-laser (337 nm) and a linear time-of-flight tube of 65 cm (Fisons Instruments, Whytenshaw, UK). Scans were accumulated over 77 laser shots, using α-cyano sinappinic acid as matrix. External calibration was realized using both gramicidin S and bovine insulin (Sigma) or internal calibration of large proteins with bovine serum albumin.

Structural alignments

The amino acid sequences of GR and FCSD were aligned based on superposition of the three-dimensional structures of each of the three domains. The domains were aligned automatically using the RIGID option of the program TURBO-FRODO (Roussel & Cambillau, 1991) with the criterion that equivalent atoms should be less than 2 Å apart. Segments of peptide chain that were spatially near but did not share the same conformation were then manually removed from the list of equivalent residues (enclosed in boxes in Fig. 7). Pairs of localized adjacent segments of equivalent residues were superposed automatically a second time using MacImldad

(Molecular Application Group, Palo Alto, California) to determine whether all equivalent residues had been identified and to locate insertions and deletions more precisely.

Supplementary material in Electronic Appendix

Extended descriptions of sequence and mass results, including tables and figures, can be found in the Electronic Appendix.

Acknowledgments

This work was supported in part by grants from the National Institutes of Health (GM21277 and GM21514), by the Concerted Research Action of the Flemish Government (120.52293), and by the Belgian National Fund for Joint Basic Research (32001891).

References

- Arieli B, Shahak Y, Taglicht D, Hauska G, Padan E. 1994. Purification and characterization of sulfide-quinone reductase, a novel enzyme driving anoxygenic photosynthesis in *Oscillatoria limnetica*. *J Biol Chem* 269:5705–5711.
- Barber MJ, Neame PJ, Lim LW, White S, Mathews FS. 1992. Correlation of X-ray deduced and experimental amino acid sequences of trimethylamine dehydrogenase. *J Biol Chem* 267:6111–6119.
- Burland V, Plunkett G III, Sofia HJ, Daniels DL, Blattner FR. 1995. Analysis of the *Escherichia coli* genome VI: DNA sequence of the region from 92.8 through 100 minutes. *Nucleic Acid Res* 23:2105–2119.
- Burns G, Brown T, Hatter K, Sokatch JR. 1989. Sequence analysis of the lpdV gene for LP of branched-chain-oxoacid dehydrogenase of *Pseudomonas putida*. *Eur J Biochem* 179:61–69.
- Chen Z, Koh M, Van Driessche G, Van Beeumen JJ, Bartsch RG, Meyer TE, Cusanovich MA, Mathews FS. 1994. The structure of flavocytochrome c sulfide dehydrogenase from a purple phototrophic bacterium. *Science* 266:430–432.
- Crestfield AM, Moore S, Stein WH. 1963. The preparation and enzymatic hydrolysis of reduced and S-carboxymethylated proteins. *J Biol Chem* 231:622.
- Cusanovich MA, Meyer TE, Bartsch RG. 1991. Flavocytochromes C. In: Mueller F, ed. *Chemistry and biochemistry of flavoenzymes*, vol II. Boca Raton Florida: CRC Press. pp 377–393.
- Dolata MM, Van Beeumen J, Ambler RP, Meyer TE, Cusanovich MA. 1993. Nucleotide sequence of the heme subunit of flavocytochrome c from the purple phototrophic bacterium, *Chromatium vinosum*. *J Biol Chem* 268:14426–14431.
- Eggink G, Engel H, Vriend G, Terpstra P, Witholt B. 1990. Rubredoxin reductase of *Pseudomonas oleovorans*. Structural relationship to other flavoprotein oxidoreductases based on one NAD and two FAD fingerprints. *J Mol Biol* 212:135–142.
- Frederick KR, Tung J, Emerick RS, Masiarz FR, Chamberlain SH, Vasavada A, Rosenberg S. 1990. Glucose oxidase from *Aspergillus niger*. Cloning, gene sequence, secretion from *Saccharomyces cerevisiae* and kinetic analysis of a yeast-derived enzyme. *J Biol Chem* 265:3793–3802.
- Frishman D, Argos P. 1995. Knowledge-based protein secondary structure assignment. *Proteins Struct Funct Genet* 23:566–579.
- Fujishiro K, Ota T, Hasegawa M, Yamaguchi K, Mizukami T, Uwajima T. 1990. Isolation and identification of the gene of cholesterol oxidase from *Brevibacterium sterolicum* ATCC 21387, a widely used enzyme in clinical analysis. *Biochem Biophys Res Commun* 172:721–727.
- Gurd FRN. 1972. Carboxymethylation. *Methods Enzymol* 25:424–438.
- Hecht HJ, Kalisz HM, Hendle J, Schmid RD, Schomburg D. 1993. Crystal structure of glucose oxidase from *Aspergillus niger* refined at 2.3 Å resolution. *J Mol Biol* 299:153–172.
- Hunter WN, Bailey S, Habash J, Harrop SJ, Helliwell JR, Aboagye-Kwarteng T, Smith K, Fairlamb AH. 1992. Active site of trypanothione reductase. A target for rational drug design. *J Mol Biol* 227:322–333.
- Karplus PA, Schulz GE. 1987. Refined structure of glutathione reductase at 1.54 Å resolution. *J Mol Biol* 195:701–729.
- Karplus PA, Schulz GE. 1989. Substrate binding and catalysis by glutathione reductase as derived from refined enzyme: Substrate crystal structures at 2 Å resolution. *J Mol Biol* 210:163–180.
- Kenney WC, Singer TP. 1977. Evidence for a thioether linkage between the flavin and polypeptide chain of *Chromatium cytochrome c₅₅₂*. *J Biol Chem* 252:4767–4772.
- Krauth-Siegel RL, Blatterspiel R, Saleh M, Schiltz E, Schirmer RH, Untucht-Grau R. 1982. Glutathione reductase from human erythrocytes. The sequence of the NADPH domain and of the interface domain. *Eur J Biochem* 121:259–267.
- Kuriyan J, Kong XP, Krishna TSR, Sweet RM, Murgolo NJ, Field H, Cerami A, Henderson GB. 1991a. X-ray structure of trypanothione reductase from *Crithidia fasciculata* at 2.4 Å resolution. *Proc Natl Acad Sci USA* 88:8764–8768.
- Kuriyan J, Krishna TSR, Wong L, Guenther B, Pahler A, Williams CH Jr, Model P. 1991b. Convergent evolution of similar function in two structurally divergent enzymes. *Nature* 352:172–174.
- Lantwin CB, Schlichting I, Kabsch W, Pai EF, Krauth-Siegel RL. 1994. The structure of *Trypanosoma cruzi* trypanothione reductase in the oxidized and NADPH reduced state. *Proteins Struct Funct Genet* 18:161–173.
- Liu XL, Scopes RK. 1993. Cloning, sequencing and expression of the gene coding NADH oxidase from the extreme thermophile *Thermoanaerobium brockii*. *Biochim Biophys Acta* 1174:187–190.
- Massey V, Muller F, Feldberg R, Schuman M, Sullivan PA, Howell LG, Mathews SG, Mathews RG, Foust GP. 1969. The reactivity of flavoproteins with sulfite. Possible relevance to the problem of oxygen reactivity. *J Biol Chem* 244:3999–4006.
- Mattevi A, Obmolova G, Sokatch JR, Betzel C, Hol WGJ. 1992. The refined crystal structure of *Pseudomonas putida* lipoamide dehydrogenase complexed with NAD⁺ at 2.45 Å resolution. *Proteins Struct Funct Genet* 13:336–351.
- Mattevi A, Schierbeck AJ, Hol WGJ. 1991. Refined crystal structure of lipoamide dehydrogenase from *Azotobacter vinelandii* at 2.2 Å resolution. A comparison with the structure of glutathione reductase. *J Mol Biol* 220:975–994.
- McPhee JR. 1956. Further studies on the reactions of disulfides with sodium sulfite. *Biochem J* 64:22–29.
- Meyer TE, Bartsch RG. 1976. The reaction of flavocytochrome c of the phototrophic sulfur bacteria with thiosulfate, sulfite, cyanide and mercaptans. In: Singer TP, ed. *Flavins and flavoproteins*. Amsterdam: Elsevier. pp 312–317.
- Meyer TE, Bartsch RG, Caffrey MS, Cusanovich MA. 1991a. Redox potentials of flavocytochromes c from the phototrophic bacteria, *Chromatium vinosum* and *Chlorobium thiosulfatophilum*. *Arch Biochem Biophys* 287:128–134.
- Meyer TE, Bartsch RG, Cusanovich MA. 1991b. Adduct formation between sulfite and the flavin of phototrophic bacterial flavocytochromes c. Kinetics of sequential bleach, recolor, and rebleach of flavin as a function of pH. *Biochemistry* 30:8840–8845.
- Mittl PRE, Schulz GE. 1994. Structure of glutathione reductase from *Escherichia coli* at 1.86 Å resolution: Comparison with the enzyme from human erythrocytes. *Protein Sci* 3:799–809.
- Muller F, Massey V. 1969. Flavin-sulfite complexes and their structures. *J Biol Chem* 244:4007–4016.
- Ross RP, Claiborne A. 1992. Molecular cloning and analysis of the gene encoding the NADH oxidase from *Streptococcus faecalis* 10C1. Comparison with NADH peroxidase and the flavoprotein disulfide reductases. *J Mol Biol* 227:658–571.
- Rossmann MG, Argos P. 1978. The taxonomy of binding sites in proteins. *Mol Cell Biochem* 21:161–182.
- Roussel A, Cambillau C. 1991. TURBO-FRODO. In: *Silicon Graphics Geometry Partners Directory*. Mountain View, California: Silicon Graphics, Inc. p 86.
- Schiering N, Kabsch W, Moore MJ, Distefano MD, Walsh CT, Pai EF. 1991. Structure of the detoxification catalyst mercuric ion reductase from *Bacillus* sp. strain RC607. *Nature* 352:168–172.
- Schulz GE, Schirmer RH, Pai EF. 1992. FAD-binding site of glutathione reductase. *J Mol Biol* 160:287–308.
- Shames SL, Kimmel BE, Peoples OP, Agabian N, Walsh CT. 1988. Trypanothione reductase of *Trypanosoma congoense*: Gene isolation, primary sequence determination and comparison to glutathione reductase. *Biochemistry* 27:5014–5019.
- Speich N, Dahl C, Heisig P, Klein A, Lottspeich F, Stetter KO, Truper HG. 1994. Adenylyl sulfate reductase from the sulfate-reducing archaeon *Archaeoglobus fulgidus*: Cloning and characterisation of the genes and comparison of the enzyme with other iron-sulfur flavoproteins. *Microbiology* 140:1273–1284.
- Stehle T, Ahmed SA, Claiborne A, Schulz GE. 1991. Structure of NADH peroxidase from *Streptococcus faecalis* 10C1 refined at 2.16 Å resolution. *J Mol Biol* 221:1325–1344.
- Thieme R, Pai EF, Schirmer RH, Schulz GE. 1981. Three-dimensional structure of glutathione reductase at 2 Å resolution. *J Mol Biol* 152:763–782.
- Van Beeumen J, Demol H, Bartsch RG, Meyer TE, Dolata MM, Cusanovich MA. 1991. Covalent structure of the diheme cytochrome subunit and amino-terminal sequence of the flavoprotein subunit of flavocytochrome c from *Chromatium vinosum*. *J Biol Chem* 266:12921–12931.
- Van Beeumen J, Van Bun S, Meyer TE, Bartsch RG, Cusanovich MA. 1990. Complete amino acid sequence of the cytochrome subunit and amino-

- terminal sequence of the flavin subunit of flavocytochrome *c* (sulfide dehydrogenase) from *Chlorobium thiosulfatophilum*. *J Biol Chem* 265:9793–9799.
- Vrielink A, Lloyd LF, Blow DM. 1991. Crystal structure of cholesterol oxidase from *Brevibacterium sterolicum* refined at 1.8 Å resolution. *J Mol Biol* 219:533–554.
- Waksman G, Krishna TSR, Williams CH Jr, Kuriyan J. 1994. Crystal structure of *Escherichia coli* thioredoxin reductase refined at 2 Å resolution. Implications for a large conformational change during catalysis. *J Mol Biol* 236:800–816.
- Wang Y, Moore M, Levinson HS, Silver S, Walsh C, Mahler I. 1989. Nucleotide sequence of a chromosomal mercury resistance determinant from a *Bacillus* sp. with broad-spectrum mercury resistance. *J Bacteriol* 171:83–92.
- Weijer WJ, Hofsteenge J, Vereijken JM, Jekel PA, Beintema JJ. 1982. Primary structure of *p*-hydroxybenzoate hydroxylase from *Pseudomonas fluorescens*. *Biochim Biophys Acta* 704:385–388.
- Wierenga RK, Drenth J, Schulz GE. 1983. Comparison of the three-dimensional protein and nucleotide structure of the FAD-binding domain of *p*-hydroxybenzoate hydroxylase with the FAD—as well as NADPH-binding domains of glutathione reductase. *J Mol Biol* 167:725–739.
- Wierenga RK, Terpstra P, Hol WGI. 1986. Prediction of the occurrence of the ADP-binding BAB-fold in proteins, using an amino acid sequence fingerprint. *J Mol Biol* 187:101–107.
- Wood D, Darlison MG, Wilde RJ, Guest JR. 1984. Nucleotide sequence of the flavoprotein and hydrophobic subunits of the succinate dehydrogenase of *Escherichia coli*. *Biochem J* 222:519–534.
- Yamanaka T. 1976. The subunits of *Chlorobium* flavocytochrome *c*. *J Biochem* 79:655–660.